Princeton Plasma Physics Laboratory

PPPL- 5011

PPPL- 5011

Parametric Dependence Of Fast-ion Transport Events On The National Spherical Torus Experiment

E.D. Fredrickson, N.N. Gorelenkov, M. Podesta, A. Bortolon, S.P. Gerhardt, R.E. Bell, A. Diallo and B. LeBlanc

MARCH, 2014

PPPL PRINCETON PLASMA PHYSICS LABORATORY

Prepared for the U.S. Department of Energy under Contract DE-AC02-09CH11466.

Princeton Plasma Physics Laboratory
Report Disclaimers

Full Legal Disclaimer

Trademark Disclaimer

PPPL Report Availability

Princeton Plasma Physics Laboratory:

http://www.pppl.gov/techreports.cfm

Office of Scientific and Technical Information (OSTI):

http://www.osti.gov/bridge

Related Links:

U.S. Department of Energy

Office of Scientific and Technical Information

Fusion Links

Parametric dependence of fast-ion transport events on the National Spherical Torus Experiment

E. D. Fredrickson, N. N. Gorelenkov, M. Podesta, A. Bortolon[1],
S. P. Gerhardt, R. E. Bell, A. Diallo, B. LeBlanc

Princeton Plasma Physics Laboratory, Princeton New Jersey 08543
[1]U Univ. of Tennessee., Knoxville, Tennessee 37916

Neutral-beam heated tokamak plasmas commonly have more than one third of the plasma kinetic energy in the non-thermal energetic beam ion population. This population of fast ions heats the plasma, provides some of the current drive, and can affect the stability (positively or negatively) of magneto-hydrodynamic instabilities. This population of energetic ions is not in thermodynamic equilibrium, thus there is free-energy available to drive instabilities, which may lead to redistribution of the fast ion population. Understanding under what conditions beam-driven instabilities arise, and the extent of the resulting perturbation to the fast ion population, is important for predicting and eventually demonstrating non-inductive current ramp-up and sustainment in NSTX-U, as well as the performance of future fusion plasma experiments such as ITER. This paper presents an empirical approach towards characterizing the stability boundaries for some common energetic-ion-driven instabilities seen on NSTX.

I. INTRODUCTION

The ability to predict the confinement and energy transfer rate of fast ions to the thermal plasma is important for accurate modeling of the beam driven currents that ITER and ST's rely upon. NSTX plasmas can have fast ion redistribution events caused by Toroidal or Global Alfvén Eigenmode (TAE/GAE) avalanches or fishbone-like Energetic Particle Modes (EPM) [1-6], periods without significant fast ion redistribution events, but with many modes, or quiescent periods with weak mode activity. The identification of plasma parameters which empirically affect the stability of modes excited by energetic particles will help to guide experiments and provide valuable input for developing theoretical models to predict the (possibly non-linear) fast ion redistribution from these instabilities.

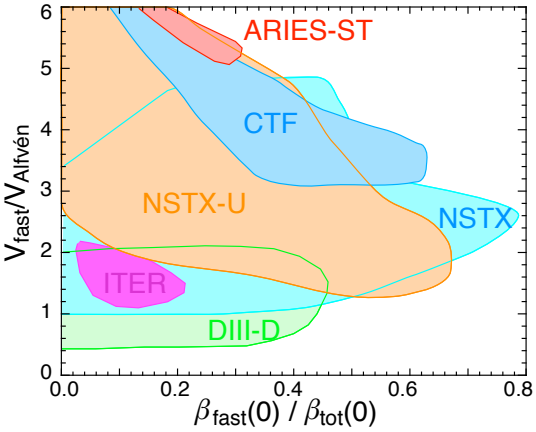

Fig. 1 Map of NSTX operational space in terms of the fast ion β normalized to the total β, and the fast ion velocity normalized to the Alfven speed.

Present theoretical understanding of TAE stability suggests parameters that might be correlated with fast-ion redistribution events. The fast ion beta is a measure of the drive for the EPM, TAE and GAE. Landau damping, an important damping mechanism, is proportional to the ion and electron thermal beta, suggesting that the dimensionless parameter $\beta_{fast}/\beta_{total}$ is an important parameter governing, at least, Alfvénic fast-ion driven instability behavior. In a similar sense, the dimensionless number giving the ratio of the fast ion injection velocity to the Alfvén speed, $V_{fast}/V_{Alfvén}$ is a measure of the fraction of fast ions in the resulting slowing-down distribution which can be resonant with the Alfvénic modes. Other parameters, more difficult to measure, such as those associated with the q-profile (*e.g.*, q_{min}), or parameters describing the fast ion distribution (*e.g.*, anisotropy) are clearly also important.

In this paper we describe the construction of a database of these plasma parameters, coupled with a characterization of the mode activity at these times. In this parameter space we will show that the existence of TAE avalanches, GAE avalanches and quiescent plasmas are constrained to certain ranges of parameters on NSTX.

II. EXPERIMENTAL APPROACH

The fast ion beta, an important parameter in this study, is not directly measured in NSTX. At present, the fast ion beta is calculated from the time evolution of plasma parameters such as density and electron temperature in each discharge, assuming only classical collisional processes. The resulting fast ion beta should be regarded as an approximate maximum, which could be degraded by many different forms of MHD activity, or possibly even by plasma turbulence. This calculation is typically done with the NUBEAM code [7] in TRANSP [8], thus, the initial part of this study was limited to NSTX shots for which TRANSP runs had been done. The database was constructed from ≈360 TRANSP runs on shots from the 2010 experimental campaign on NSTX.

The database was constructed by dividing each TRANSP run into 50ms intervals, starting at 150ms and characterizing the type of MHD activity in the interval. Typically by 150ms NSTX plasmas have reached a plasma current of ≈ 0.6MA to 0.7MA, and fast ion confinement is reasonably good. The 50ms time interval is several fast-ion slowing down times, and is typically comparable to the timescale for evolution of MHD phenomena. The average density, energy stored in the fast ion population, plasma total stored energy, and maximum beam injection voltage for each 50ms interval are extracted from the data stored in the TRANSP output files. The plasma density, together with the magnetic field on axis, is used to calculate an effective Alfvén velocity and the beam voltage is used to calculate the maximum beam ion velocity, from which the normalized fast ion velocity, $V_{fast}/V_{Alfvén}$ is calculated.

The MHD activity in each 50ms interval was classified as having TAE avalanches, bursting TAE, constant-amplitude TAE, EPMs, global Alfvén eigenmode avalanches, Abrupt Large Events (ALEs) [9-11] or plasmas quiescent in the TAE and lower frequency range. As the kink modes are believed to redistribute fast ions, intervals with kink modes in addition to the fast-ion driven MHD events were counted as 'kinks'. Intervals with GAE avalanches were counted independently of the other classification of the interval.

The distinction between TAE avalanches, EPMs and ALEs is not as unambiguous on NSTX as it is on conventional aspect ratio tokamaks. The low field, high density and unbalanced co-injected beams typically result in a core rotation frequency comparable to the TAE gap frequency. For modes with moderate toroidal mode number, n, the Doppler corrected TAE frequency is typically near zero in the plasma frame near the magnetic axis, allowing direct

coupling of TAE to EPM or other core MHD modes. That is, the TAE frequency range overlaps the frequency range of EPMs and kink modes.

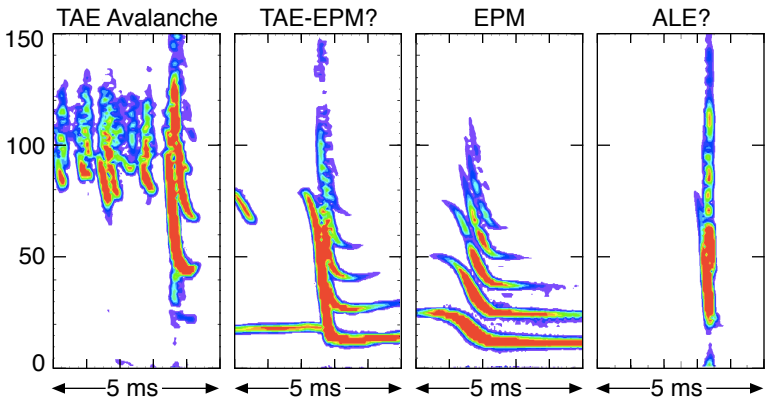

Fig. 2a) spectrogram showing TAE avalanche, b) spectrogram showing hybrid TAE avalanche and EPM, c) spectrogram of EPM avalanche and d) spectrogram of ALE.

Representative examples of a TAE avalanche, EPM and ALE are shown in Fig. 2. In the first frame, the strong burst of activity is preceded by weaker modes with frequencies consistent with the TAE frequencies calculated by the NOVA code [12-14]. The modes in the strong burst chirp down to low frequencies, but at mode onset, they are in the TAE frequency range. In the second frame is an example of a mode burst with both TAE avalanche and EPM characteristics. The mode onset frequency appears to be in the TAE gap, the modes chirp to low frequency, but the post-burst frequency evolution is more consistent with ideal kink-like modes, suggesting that the TAE couple to (and sometimes trigger) a core kink-like mode. The third frame shows a typical EPM avalanche where the mode onset frequency is well below the (core) TAE frequency band and the harmonic spacing is consistent with kink-like modes. In the final frame is a burst reminiscent of the Abrupt Large Events reported on the JT-60U experiment. The spectrogram does suggest very rapid downward frequency chirping, and the ALE on NSTX are likely just an example of extremely fast chirping TAE avalanches.

III. EXPERIMENTAL RESULTS

Some data from the database are shown in Fig. 3. Each point in the figure represents a 50 ms interval in one of the 360 shots comprising the database. The color of the point indicates the type of instability dominant in that interval. The horizontal axis is the ratio of the fast ion beta, β_{fast}, to the total plasma beta, β_{total}. The vertical axis is the ratio of the birth velocity of the full-energy beam ions normalized to an average Alfvén speed. The Alfvén speed is calculated using the magnetic field on the magnetic axis, and the line-average of the plasma electron density inside the pedestal (from a major radius of 0.3m to 1.4m). Other choices for the axis, for example, using more core-localized values, would result in small qualitative changes to this

graph, but there is probably a high degree of self-similarity in these NSTX discharges that would make the results insensitive to those changes.

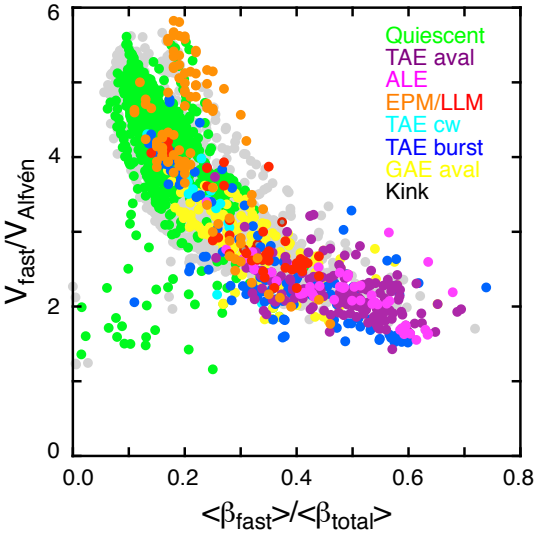

Fig. 3. Existence plot for a variety of types of MHD activity.

Each point in Fig. 3 shows the ratio of fast ion velocity to an effective Alfvén speed where the fast ion velocity is calculated at the maximum injection energy. The neutral beams on NSTX also inject substantial power in fast ions at the half and third energies. Together, the injected energetic ions collisionally slow down in the plasma, resulting in a non-thermal slowing down distribution that extends downward to some small multiple of the ion temperature, or about 10% of the injection energy, at which point they are considered as part of the thermal ion distribution. Thus, each point should be viewed as an upper limit, and that the non-thermal fast ion distribution extends downward to roughly 1/3 the velocity indicated by each point (for nearly all of the data, the injection energy was 90 keV).

Generally, NSTX shots evolve, starting from the lower right of Fig. 3 and moving upwards and to the left as the plasma density increases. The increasing density lowers the Alfvén speed, increasing $V_{fast}/V_{Alfvén}$, and the higher density decreases the fast-ion slowing-down time, dropping the fast-ion stored energy. At the same time, the density rise generally coincides with an increase in the thermal plasma stored energy or β_{total}. Thus, there can be hidden correlations in these figures as, for example, points in the lower right would tend to have elevated q_{min} and typically core shear reversal.

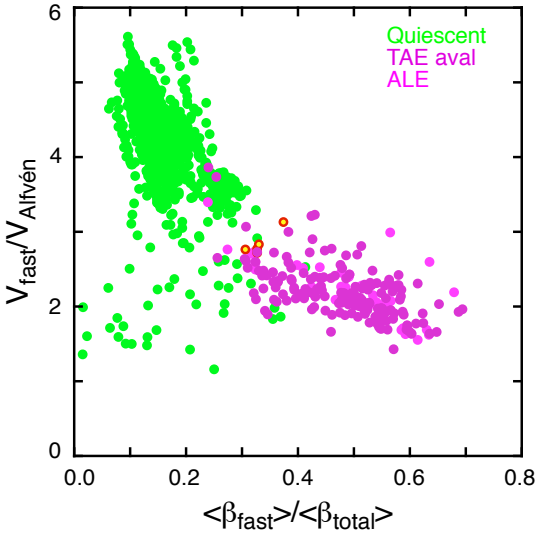

Fig. 4. Distribution of quiescent shots (green), and shots with TAE avalanches (purple), Abrupt Large Events (magenta).

The quiescent discharge periods, and periods with TAE avalanches and ALEs are well localized in this parameter space. In Fig. 4 are plotted the quiescent period data (green points). There does not seem to be a strong dependence on normalized fast

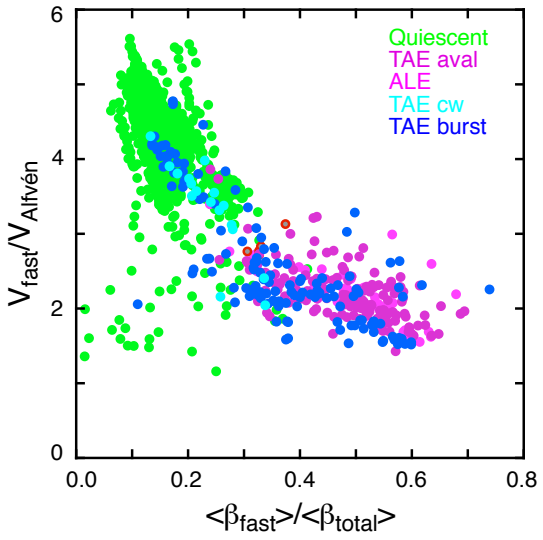

Fig. 5. Distribution of shots with bursting and chirping TAE (blue) and continuous amplitude TAE (cyan).

ion velocity, but quiescent plasmas mostly have a ratio of fast-ion stored energy to total stored energy of less than ≈ 30%. Conversely, the TAE avalanches and ALE events occur where that ratio, $\beta_{fast}/\beta_{total} > 0.3$. Again, within this dataset, there does not seem to be a significant dependence on the $V_{fast}/V_{Alfvén}$. Even the L-mode avalanches, with lower voltage beams (60-70 keV), fall into the same region.

Many shots have TAE activity below the threshold for causing measurable transient drops in the neutron rate. These tend to be distributed fairly uniformly as can be seen in Fig. 5. Here, the presence of bursting and chirping TAE are indicated by blue points and TAE with a more continuous amplitude evolution are indicated in cyan. The bursting and chirping TAE overlap the TAE avalanching region, but also extend into the parameter space where quiescent plasmas are found. The continuous TAE mostly overlap the quiescent regime and appear to be weaker modes.

The second type of instability responsible for fast ion redistribution events are Energetic Particle Modes (EPM). These instabilities are not eigenmodes of the plasma, excited by a non-thermal particle population, but exist only in the presence of an energetic particle (ion) population. Their frequencies are a characteristic of the energetic fast ion population. There are many qualitatively different low frequency chirping modes that are classified as EPMs on NSTX. However, a large fraction of these bursts are of the types shown in Figs. 6 and 7. In Fig. 6a are shown typical EPM bursts as seen in the latter part of the discharge, although bursts like these may appear early, as well. They resemble the classical fishbone modes seen on

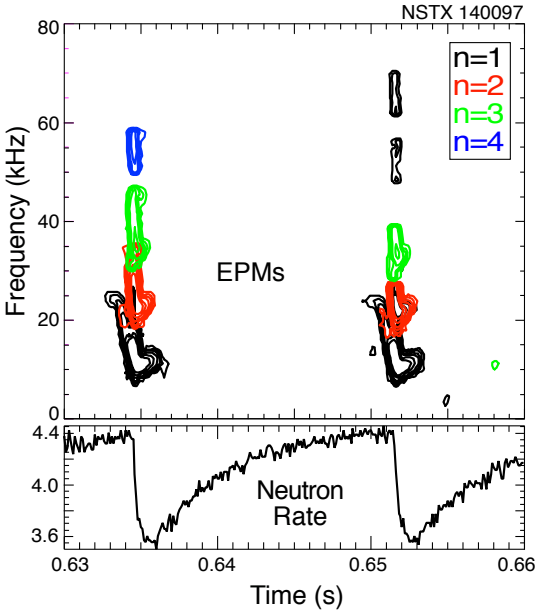

Fig. 6. Fishbone-like EPMs in later part of NSTX discharge. Coupling of n=1 to higher n's is commonly seen.

conventional tokamaks, and like those, appear when q_{min} or q(0) is near unity. They may be accompanied by substantial, but transient, drops in the neutron rate as seen in Fig. 6b. Typically on NSTX, the bursts involve multiple toroidal mode numbers, as indicated in Fig. 6a by the colored contours.

In Fig. 7 is shown an example of the second common form of EPM. The multiple toroidal mode numbers, and the relatively small frequency chirps are very similar to the EPMs in Fig. 6. However, these EPMs, which are typically seen early in the discharge when q_{min} is still elevated, convert to long-lived modes [15,16]. As the duration of the long-lived mode varies considerably, the distinction between the types can be somewhat arbitrary.

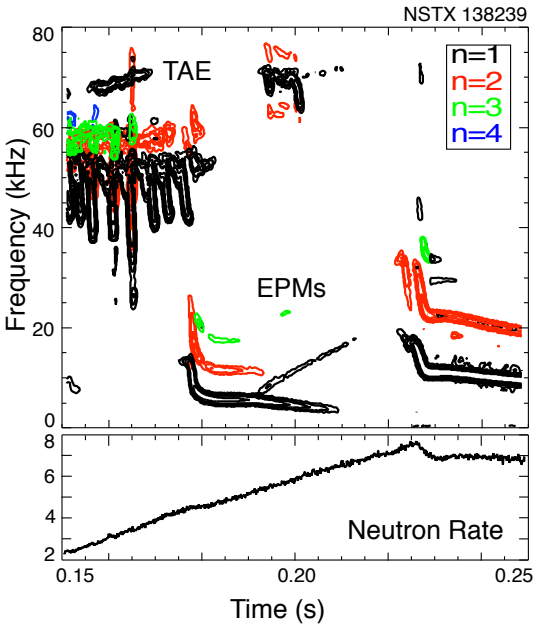

Fig. 7. Fishbone-like EPMs coupled to long-lived modes; a) spectrogram of Mirnov coil signal, b) neutron rate.

In Fig. 8 are shown the EPM points (orange, red and blue), overlaid on the quiescent regime (green points) and kink-like modes (grey). Here, the two subgroups of EPM from above are separately identified. In blue are EPMs which closely resemble classical fishbones and in red are EPMs coupled to the long-lived mode. The orange points represent EPMs which are not easily sorted into the above categories. EPMs and kinks are of course related as the EPM is, generically, a stable kink mode destabilized by a resonance with fast ions. The fast frequency chirp of EPMs is used to discriminate between them and kink modes. However, many long-lived kinks on NSTX begin with a quick downward frequency chirp similar to the long-lived modes on MAST, which suggests that fast ion resonances may play a role in maintaining their saturated state.

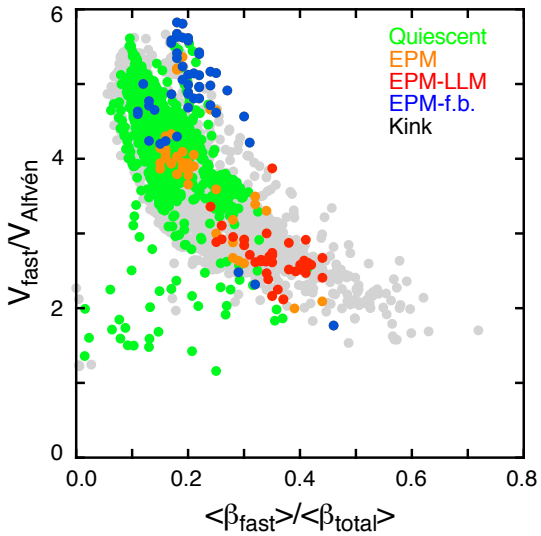

Fig. 8. Energetic Particle Mode (EPM) events (orange) are seen over most of NSTX operating space, as are low frequency kink-like modes (grey).

The EPMs tend to be more core-localized than the

TAE, thus $\beta_{fast}(0)/\beta_{total}(0)$ might be a more appropriate parameter than one using volume-averaged β's. In Fig. 9 is an existence plot for the EPM against the central and volume averaged ratios of the fast ion to the total pressures. The first observation is that these two parameters are fairly well correlated, which indicates that the ratio of the peaking factors for the fast ion pressure profile and total pressure profile are correlated. In terms of the core parameters, EPM appear to be absent for $\beta_{fast}(0)/\beta_{total}(0) < 0.2$, or similarly, for $<\beta_{fast}>/<\beta_{total}> < 0.1$. The solid line indicates where the fast-ion pressure peaking factor is twice that of the total pressure. The upper and lower dashed lines correspond to peaking factor ratios of 2.5 and 1.5, respectively.

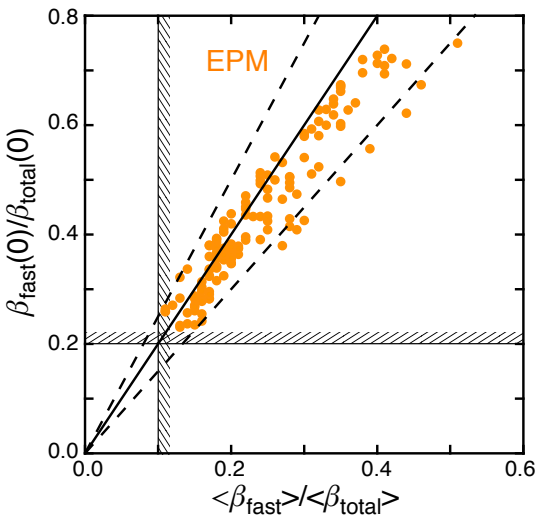

Fig. 9. EPM existence plot in the parameter space of $\beta_{fast}(0)/\beta_{total}(0)$ vs $<\beta_{fast}>/<\beta_{total}>$. Solid line indicates β_{fast} peaking factor twice β_{total} peaking factor.

This choice of normalized fast ion velocity and normalized fast ion beta also works reasonably well for predicting conditions under which Global Alfvén Eigenmode (GAE) avalanches are seen. GAE avalanches have not, so far, resulted in measurable neutron rate drops, but there are direct and indirect indications of fast ion redistribution due to GAE avalanches. In Fig. 10 is shown the region where GAE avalanches are found. They extend down to lower $\beta_{fast}/\beta_{total}$ than the TAE avalanches, and there may also be a cutoff for $V_{fast}/V_{Alfvén}$ greater than ≈3.5. Predictive TRANSP runs were done to simulate NSTX-U performance using the neutral beam parameters and machine parameters (plasma current, toroidal field, vacuum vessel configuration) expected for NSTX-U. The TRANSP runs explored a range of parameters, including different combinations of neutral beam sources, and scans of density and toroidal field. Using those predictive TRANSP runs, we can compare the expected operational space of NSTX-U with the NSTX data presented above. In Fig. 11 is shown the

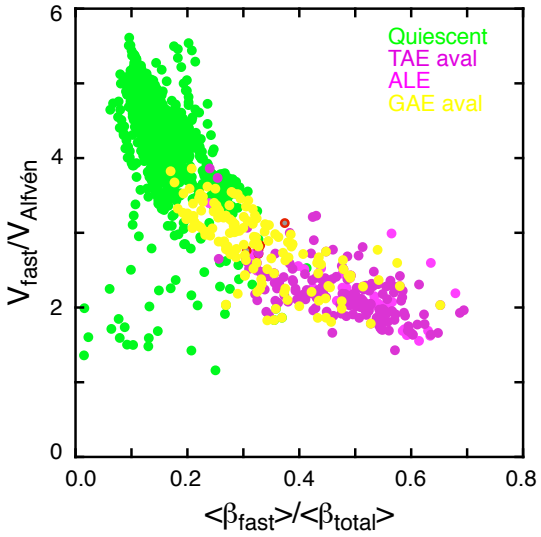

Fig. 10. Yellow points indicate parameters for which GAE avalanches were seen.

data from these TRANSP runs, analyzed in the same manner as above. Data from the NSTX-U TRANSP runs is shown in black, and is overlaid by the quiescent and TAE avalanching data points from NSTX. As can be seen, NSTX-U should be able to access parameters which were found to be quiescent on NSTX, as well as parameters where TAE avalanching might be expected. NSTX-U will also extend the operational space to much lower $V_{fast}/V_{Alfvén}$.

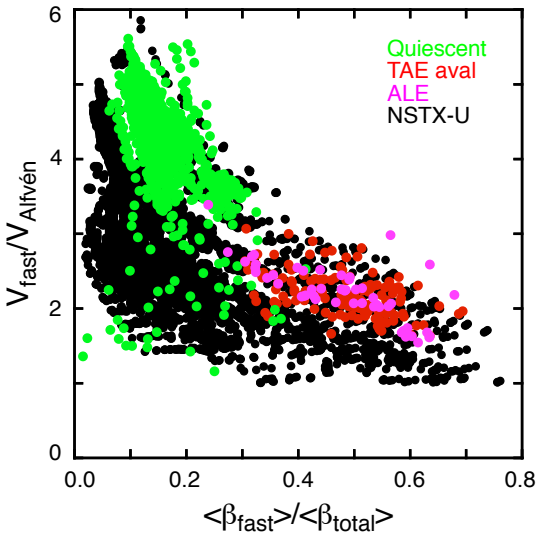

Fig. 11. Operational space for NSTX-U as predicted with TRANSP (black), overlaid by data from NSTX.

IV. Scaling of the transient neutron rate drops

The neutron rate transiently drops during each TAE avalanche or EPM event. The neutron rate drop is due to fast ion redistribution, fast ion losses and to energy transferred from the fast ions through the mode to the thermal plasma. A prediction of the neutron rate drop is complicated, and depends on the structure of the modes, the mode frequency and amplitude evolution, the initial fast ion distribution, and other parameters. Here, we look at the empirical scaling of neutron rate drops *versus* a single parameter, the peak mode amplitude as measured by a Mirnov coil. In Fig. 12 is shown a plot of the drop in neutron rate vs the peak amplitude of the TAE avalanche. Here, the red points correspond to TAE avalanches, and the purple points to bursts identified as ALE. The neutron rate drops follow an offset-linear scaling with mode amplitude, suggesting an amplitude threshold for the onset of the avalanche. This is consistent with fast ion transport simulations during avalanches, which also found a threshold in amplitude, both for significant fast ion energy loss and redistribution, and a higher threshold still for fast ion losses. As the TAE avalanche amplitude drops, the change in neutron rate becomes smaller, until the neutron rate change becomes comparable to the noise

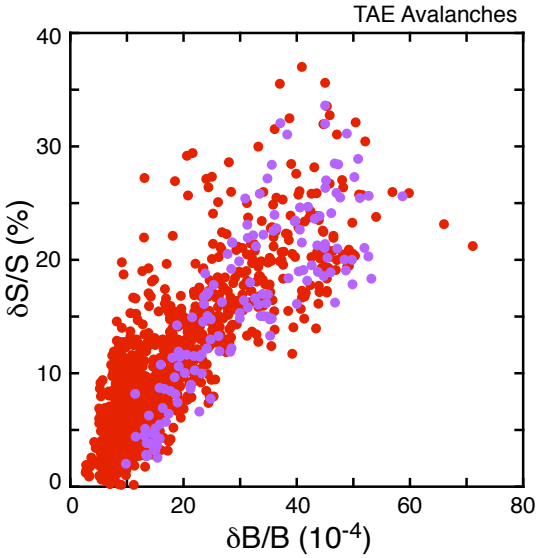

Fig. 12. Drop in neutron rate vs. peak edge magnetic fluctuation amplitude for TAE avalanches (red) and ALE (purple).

level.

In Fig. 13 is shown the scaling of neutron rate drops due to fishbone-like EPM and EPM coupled to long-lived modes, together with the scaling for TAE bursts (now shown in green) as in Fig. 12. The peak EPM edge magnetic fluctuation level tends to be larger that that for TAE avalanches for similar drops in the normalized neutron rate. There is enough scatter in the data to make it clear that parameters in addition to the edge mode amplitude play a role in the magnitude of the neutron rate drop. The scaling of the neutron rate drop with edge magnetic fluctuation amplitude is similar for the two types of fishbone-like EPMs, although there is considerably more scatter for the EPM coupled to the long-lived mode, perhaps reflecting more variability in the plasma conditions at the time of these events.

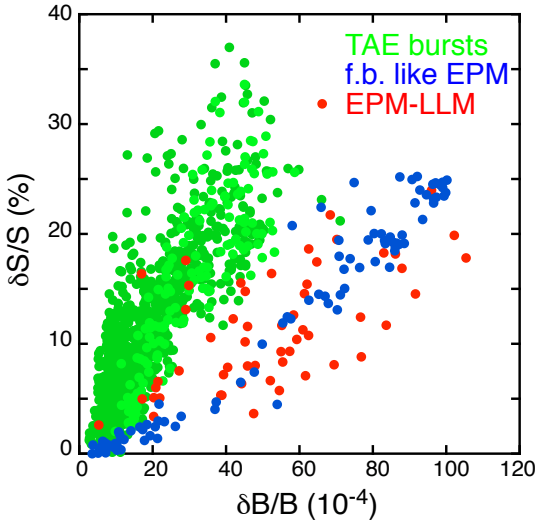

Fig. 13. Scaling of neutron rate drops with edge magnetic fluctuation amplitude for TAE (green), fishbone-like EPM (blue) and EPM coupled to long-lived modes (red).

V. Summary

The dependence of energetic particle driven mode activity on plasma global parameters has been studied in NSTX. On NSTX, two fast ion instabilities are predominantly responsible for fast ion redistribution events, the TAE avalanches and fishbone-like Energetic Particle Modes. Understanding the conditions under which beam-driven instabilities arise, and the extent of the resulting perturbation to the fast ion population, is important for predicting and eventually demonstrating non-inductive current ramp-up and sustainment in NSTX-U, as well as for predicting the performance of future fusion plasma experiments such as ITER. A database has been constructed for each 50ms interval from a representative selection of ≈360 shots. The database includes some basic, global plasma parameters, as well as the identification of the dominant mode activity in each interval. It has been shown that for this NSTX data set, TAE avalanching is only seen when the calculated $\beta_{fast}/\beta_{total} > 0.3$, and conversely, that quiescent plasmas are only seen for $\beta_{fast}/\beta_{total} < 0.3$.

The fast ion losses for both TAE avalanches and EPMs scale roughly linearly with mode amplitude as measured with Mirnov coils. This linear scaling is similar to what has been

reported for losses resulting from TAE bursts on TFTR [17], although the offset-linear scaling seen here for TAE avalanches was not seen on TFTR.

Acknowledgements

The authors would like to express their appreciation to the NSTX team for performing the experiments from which this data was collected. This manuscript has been authored under U.S. DoE Contract Number DE-AC02-09CH11466.

Bibliography

[1] *Fast-ion energy loss during TAE avalanches in the National Spherical Torus Experiment*, E D Fredrickson, , N.A. Crocker, D.S. Darrow, N.N. Gorelenkov, G.J. Kramer, S. Kubota, M. Podesta, R.B. White, A. Bortolon, S.P. Gerhardt, R.E. Bell, A. Diallo, B. LeBlanc, F.M. Levinton and H. Yuh, Nucl. Fusion **53** (2013) 013006

[2] "*Bounce precession fishbones in the National Spherical Torus Experiment*", E D Fredrickson, L Chen, R B White, Nucl. Fusion 43 (2003) 1258.

[3] *Wave driven fast ion loss in the National Spherical Torus Experiment,* E.D. Fredrickson, C.Z. Cheng, D. Darrow, G. Fu, N.N. Gorelenkov, G Kramer, S S Medley, J. Menard, L. Roquemore, D. Stutman[1], R. B. White, Phys. of Plasmas 10 (2003) 2852.

[4] *Experimental studies on fast-ion transport by Alfvén wave avalanches on the National Spherical Torus Experiment*, M. Podestà, W. W. Heidbrink, D. Liu, E. Ruskov, R. E. Bell, D. S. Darrow, E. D. Fredrickson, N. N. Gorelenkov, G. J. Kramer, B. P. LeBlanc, S. S. Medley, A. L. Roquemore, N. A. Crocker, S. Kubota, and H. Yuh, Phys. of Plasmas 16 (2009) p056104.

[5] *Stochastic orbit loss of neutral beam ions from NSTX due to toroidal Alfven eigenmode avalanches*, D S Darrow, N. Crocker, E.D. Fredrickson, N.N. Gorelenkov, M. Gorelenkova, S. Kubota, S.S. Medley, M. Podestà, L. Shi and R.B. White, Nucl. Fusion **53** (2013) 013009

[6] "*Study of chirping TAEs on the National Spherical Torus Experiment*", M. Podestà, R.E. Bell, A. Bortolon, N.A. Crocker, D.S. Darrow, A. Diallo, E.D. Fredrickson, G.-Y. Fu, N.N. Gorelenkov, W.W. Heidbrink, G.J. Kramer, S. Kubota, B.P. LeBlanc, S.S. Medley and H. Yuh, , Nucl. Fusion **52** (2012) 094001.

TRANSP/NUBEAM

[7] R V Budny, Nucl. Fusion **34** (1994) 1247.

[8] A. Pankin, D. McCune, R. Andre *et al*., Comp. Phys. Comm. **159**, (2004) 157-184.

ALE

[9] K. Shinohara, Y. Kusama, M. Takechi, A. Morioka, M. Ishikawa, N. Oyama, K. Tobita, T. Ozeki, S. Takeji, S. Moriyama, T. Fujita, T. Oikawa, T. Suzuki, T. Nishitani, T. Kondoh, S. Lee, M. Kuriyama, JT-60 Team, G.J. Kramer, N.N. Gorelenkov, R. Nazikian, C.Z. Cheng, G.Y. Fu,A. Fukuyama, Nucl. Fusion **41** (2001) 603.

[10] *Recent progress of Alfvén eigenmode experiments using N-NB in JT-60U tokamak*, K. Shinohara, M. Takechi, M. Ishikawa, Y. Kusama, A. Morioka, N. Oyama, K. Tobita, T. Ozeki, the JT-60 Team, N.N. Gorelenkov, C.Z. Cheng, G.J. Kramer and R. Nazikian, Nucl. Fusion **42** (2002) 942.

[11] *Energetic particle physics in JT-60U and JFT-2M*, K Shinohara, M Takechi, M Ishikawa1, Y Kusama, K Tsuzuki, K Urata, H Kawashima, K Tobita, A Fukuyama, C Z Cheng, D S Darrow, G J Kramer, N N Gorelenkov, R Nazikian, Y Todo, Y Miura and T Ozeki, Plasma Phys. Control. Fusion **46** (2004) S31–S45

NOVA

[12] *Kinetic Extensions of Magnethydrodynamic Models for Axisymmetric Toroidal Plasmas*, C. Z. Cheng, Phys. Reports (A Review Sec. of Phys. Letters.), 211, 1-51 (February, 1992)

[13] "*Fast particle finite orbit width and Larmor radius effects on low-n toroidicity induced Alfvén eigenmode excitation"* , N. N Gorelenkov, C. Z. Cheng, and G. Y. Fu, Phys. Plasmas **6** (1999) 2802.

[14] *Interpretation of core localized Alfvén eigenmodes in DIII-D and Joint European Torus reversed magnetic shear plasmas"*, G. J. Kramer, R. Nazikian, B. Alper, M. de Baar, H. L. Berk, G.-Y. Fu, N. N. Gorelenkov, G. McKee, S. D. Pinches, T. L. Rhodes, S. E. Sharapov, W. M. Solomon,M. A. van Zeeland, Phys. Plasmas **13** (2006) 056104.*long lived mode*

[15] M.P. Gryaznevich, S.E. Sharapov, M. Lilley, S.D. Pinches, A.R. Field, D. Howell, D. Keeling, R. Martin, H. Meyer, H. Smith, R. Vann, P. Denner, E. Verwichte and the MAST Team, Nucl. Fusion **48** (2008) 084003.

[16] I.T. Chapman, M.-D. Hua, S.D. Pinches, R.J. Akers, A.R. Field, J.P. Graves, R.J. Hastie, C.A. Michael and the MAST Team, *Nucl Fusion* 50 (2010) 045007

TFTR losses

[17] *Losses due to Alfven Modes in TFTR*, D.S. Darrow, S.J. Zweben, Z. Chang, C.Z. Cheng, M.D. Diesso, E.D. Fredrickson, E. Mazzucato, R. Nazikian, C.K. Phillips, S. Popovichev, M.H. Redi, R.B. White, J.R. Wilson, K.-L. Wong, Nucl. Fusion, Vol. **37**, (1997) 939.

The Princeton Plasma Physics Laboratory is operated
by Princeton University under contract
with the U.S. Department of Energy.

Information Services
Princeton Plasma Physics Laboratory
P.O. Box 451
Princeton, NJ 08543

Phone: 609-243-2245
Fax: 609-243-2751
e-mail: pppl_info@pppl.gov
Internet Address: http://www.pppl.gov